Underwater Laser Serial Imaging Using Compressive Sensing and Digital Mirror Device

Bing Ouyang*[a], Fraser R. Dalgleish[a], Frank M. Caimi[a], Thomas E. Giddings[b], Joseph J. Shirron[b], Anni. K. Vuorenkoski[a], Gero Nootz[a], Walter Britton[a], Brian Ramos[a]

a. Florida Atlantic Univ./HBOI, 5600 US 1, Fort Pierce, FL, USA 34946
b. Metron Inc.1818 Library Street Suite 600, Reston, VA, USA 20190

ABSTRACT

The compressive sensing (CS) theory has drawn great interest in signal processing community in recent years and led to new image acquisition techniques in many different fields. This research attempts to develop a CS based underwater laser serial imaging system. A Digital Mirror Device (DMD) based system configuration is proposed. The constraints due to scattering medium are studied. A multi-scale measurement matrix design, the "model-assisted" image reconstruction concept and a volume backscattering reduction technique are proposed to mitigate such constraints. These concepts are also applicable to CS based imager in other scattering environment such as fog, rain or clouds. Simulation results using a modified imaging model developed by HBOI and Metron and experimental results using a simple optical bench setup are presented. Finally the proposed technique is compared with traditional laser line scan (LLS) design and other structured illumination based imager.

Keywords: laser imaging, underwater imaging, compressive sensing, scattering medium, spatial light modulation

1. EXISTING EXTENDED RANGE UNDERWATER IMAGERS

To date the most highly regarded extended range underwater laser imaging technique is the laser line scan (LLS) system [1]. The LLS imagers operate in serial mode, where scanning optics, electronics and mechanical components function to ensure that both the laser and telescopic receiver synchronously scan over a wide target region in line-by-line fashion. At each target element, a "bucket" photon detector such as a Photomultiplier tube (PMT) records the photon counts from target reflections and generates output as an analog voltage. A high-speed ADC digitizes the PMT output voltage to produce an uncompressed image of the scene. The image can then be compressed using codecs such as JPEG. Opto-mechanical components such as a high precision prism and aperture assemblies are needed to ensure the proper operation of the system. Such components lead to high system bill of materials (BOM) and the many moving parts can reduce system reliability. Furthermore, the bulky optical and mechanical parts limit the compactness of the system packaging. Future extended range laser imagers for undersea imaging applications will need to be extremely compact to be compatible with current and future classes of man-portable autonomous underwater vehicle (AUV).

In pursuit of more compact, reliable system concepts with lower BOM, a structured illumination parallel laser imaging approach was recently described [2]. A DMD was used to spatially modulate a single pulse laser and split it into multiple beams that were separated by a pre-defined distance. Such separation ensured that there was little overlap between beams after spreading in turbid water. A range-gated camera was proposed to acquire the image. Finally, an image synthesis process was used to construct the final uncompressed image (Figure 1).

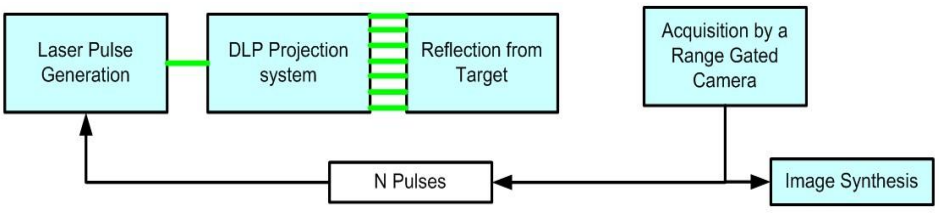

Figure 1 Structured Illumination based Imager [2]

However, this technique shares the same image acquisition paradigm as the laser line scan system in that the raw uncompressed data is first acquired and then a codec such as JPEG or JPEG2000 is used to compress the data before to be stored in the storage device (Figure 2).

Fig. 2 Image Acquisition Paradigm for LLS and Structured Illumination Technique

In recent years, the compressive sensing theory has drawn considerable interest in various signal acquisition applications. However, so far, there was not any reported development of CS based underwater laser imagers. This work is intended to study the feasibility of such an application. As a first attempt, only imaging of a static scene is considered.

2. COMPRESSIVE IMAGING

2.1. Fundamentals of Compressive Sensing

Compressive sensing (CS) is a framework for the simultaneous sampling and compression of sparse (therefore compressible) signals using incomplete, non-adaptive linear measurements [3-6]. An *N*-pixel signal $X=\{X(n), n=1,2,\cdots N\}$ is said to be *K-sparse* if there exists an *N*-dimensional sparsifying basis $\Psi=\{\psi_1,\psi_2\cdots,\psi_N\}$ and $X=\Psi a$, where the $N\times 1$ vector a contains $K<<N$ non-zero entries. CS theory states that if there is such *K*-sparse basis exists for *X*, then *X* can be recovered with overwhelming probability using more than $M=O(K\log N)$ incoherent linear measurements: $Y=\Phi X=\Phi\Psi a$, where Y is a $M\times 1$ vector and Φ is a $M\times N$ matrix that is incoherent with the sparsifying matrix Ψ [3] (Figure 3).

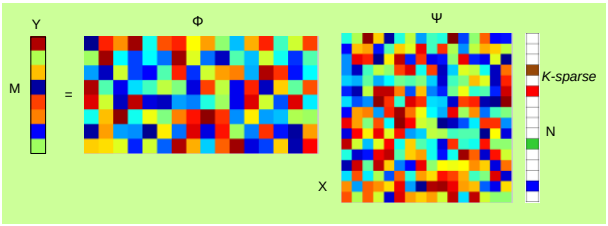

Figure 3 Incoherent Linear Measurements of *K*-sparse Signal [9]

The matrix Φ is referred to as the *measurement matrix* [9]. The incoherent property can be satisfied if the maximum magnitude of the elements of $\Phi\Psi$ is small [6]. This condition can be achieved if Φ is a random basis such as pseudo-random sequence, Bernoulli binary vectors or scrambled block Hadamard Ensemble [7],[15]; whereas *K*-sparse sparsifying basis Ψ exists for many signal types, for example, natural images are sparse in Fourier, DCT or wavelet domain, a property exploited in the compression standards such as JPEG and JPEG2000. The l_1 norm minimization [5] can recover *a* (therefore *X*) from the measurements *Y:*

$$\begin{aligned}&\hat{\alpha}=\arg\min\|a\|_1\\&subject\ to\quad Y=\Phi\Psi a\end{aligned}\tag{1}$$

where $\|a\|_1=\sum_{i=1}^{N}|a_i|$ is the l_1 norm of a. Such an optimization problem is called *basis pursuit* [5].

The application of CS theory in image and video applications, or Compressive Imaging (CI) is one area drawn extensive interests. In addition to the aforementioned sparsifying basis, the image gradient sparsity can also be exploited via minimization of the image total variation (TV). For a digital image *X*, at pixel location x_{ij}, the discrete gradient $D_{ij}(X)$ is defined as [12]:

$$\begin{aligned}&D_{ij}(X)=\begin{pmatrix}D_{h;ij}(X)\\D_{v;ij}(X)\end{pmatrix}\\&D_{h;ij}(X)=x_{i+1,j}-x_{i,j}\qquad D_{v;ij}(X)=x_{i,j+1}-x_{i,j}\end{aligned}\tag{2}$$

Then the TV of *X* is the sum of the magnitudes of $D_{ij}(X)$ at every point in *X*:

$$TV(X) = \sum_{ij} \sqrt{D_{h;ij}(X)^2 + D_{v;ij}(X)^2} \tag{3}$$

TV minimization with quadratic constraints has been shown to provide better visual quality than that l_1 optimization [12] when recovering images from noisy observations:

$$\begin{aligned} &\min TV(X) \\ &subject\ to \quad \left\|\Phi X - Y\right\|_2 \le \varepsilon \end{aligned} \tag{4}$$

Candes and Romberg summarized seven different optimization problems to reconstruct data from compressive sensing measurements in their *l1_MAGIC* software package for solving the inverse problem of compressive sensing [14].

2.2. Compressive Imaging Applications

Rice one pixel camera was one of the earlier successful implementations of Compressive Imaging [8-9]. The core of the design is a binary spatial light modulator (SLM) based on Digital Mirror Device (DMD) from Texas Instruments.

DMD consists of millions of electrostatic actuated micro-mirrors that can be individually controlled to reflect light to one of two distinctive directions to modulate incoming light source in binary mode (Figure 4). While mainly used as display devices in DLP® TV or data projector, DMD also was used as an SLM device due to its high distinguish ratio and fast switching speed (up to 32K patterns per second) [16].

(a) Two DMD mirror-pixels [16] (b) DLP™ projection system [23]

Figure 4 Digital Mirror Device and DLP™ System

In the Rice one-pixel camera project, the measurement matrices Φ consisted of *M* different $n \times n$ binary random patterns. A light emitting diode (LED) illuminated the target; the target reflection was focused onto a DMD. The m^{th} random patterns $\{\phi_m, m = 1,2...M\}$ were loaded onto DMD to modulate the target reflection. The modulated light was focused on to a photodiode. The photodiode output was digitized via an ADC to provide the m^{th} measurement $\{y_m, m = 1,2...M\}$. An optimization process such as basis pursuit then reconstructed the image *X* using the *M* binary measurement matrices $\Phi = \{\phi_m\}$ and the *M* measurements $Y = \{y_m\}$ (Figure 5). Even though no detail was given, an active illumination based one-pixel camera was also alluded to in [9].

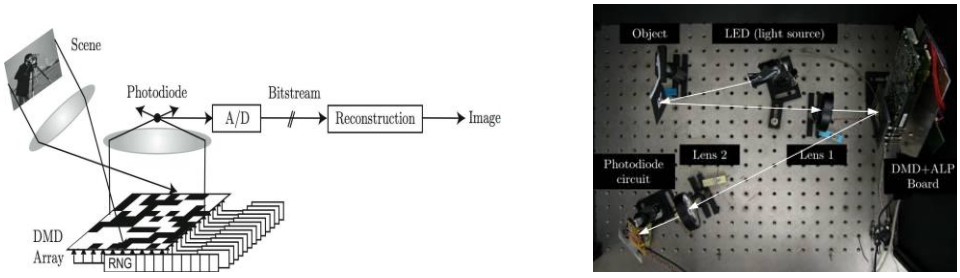

(a) Architecture [8] (b) Optical Bench Setup [8]

Figure 5 Rice One Pixel CS Camera

CS theory has been adopted in other imaging applications too. Ma proposed CS based single-pixel multiple times (SPMT) imaging for aerial remote sensing [17]. Lustig et al. adopted CS for rapid magnetic resonance imaging [18]. Baraniuk and Steeghs applied CS in Radar imaging [19].

3. CS UNDERWATER LASER IMAGER

3.1. Basic System Concept

The initial design of the proposed CS underwater laser imager is essentially a hybrid of aforementioned laser line scan system, structured illumination as well as the Rice one-pixel camera (Figure 6). At the illuminator, the laser beam is focused on to a solid-state SLM device such as DMD. A series of binary measurement matrices $\{\phi_m\}$ are loaded onto the DMD to modulate the laser; the dither patterns are then projected onto the target surface. At the receiver, like the LLS system, a PMT measures the total photon reflection corresponding to each different dither pattern. The PMT output voltages are digitized via an ADC to generate the measurements $\{Y_m\}$. $\{\phi_m\}$ and $\{Y_m\}$ are used as inputs to a TV minimization based optimization process to reconstruct the image. The transmitter and receiver could be co-located like a mono-static LLS system or on different platforms like a bi-static LLS imager.

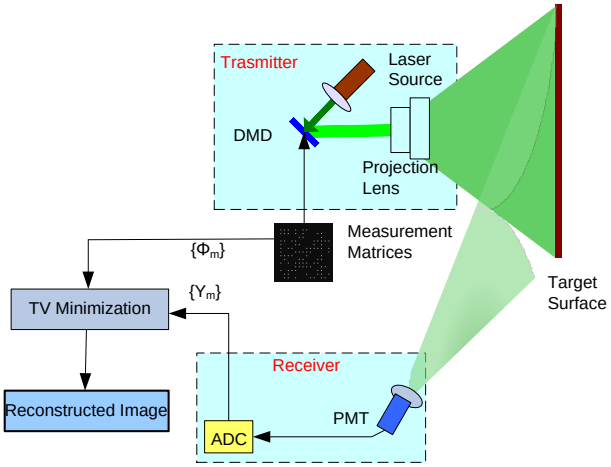

Figure 6 Initial CS Underwater Laser Imager concept

However, simulation based on this configuration did not yield satisfactory result. Compared to the over-the-air scenarios, the main challenge for underwater laser imagers is the beam spreading due to dispersive nature of the water body. As in any CS based applications, the measurement matrix is a critical component. The beam spreading causes two issues. First, since the existing binary CS measurement matrices all contain dense dither patterns (Figure 7(a)), the details in the dither pattern will be eliminated after propagating in the water medium (Figure 7(b)). Secondly, the original binary patterns enter the water is not the patterns that modulating the target plane.

(a)Original (b) At 5 Att. Len

Figure 7 Dither Pattern in Turbid Water

As detailed in subsequent sections, the proposed design overcame these challenges through two key contributions: a new measurement matrices design and radiative transfer model based image reconstruction process.

3.2. Multi-scale Measurement Matrix Design

In a multi-scale binary dither pattern (Figure 8), the dither pattern is divided into small blocks of pre-defined size. Only one "on" pixel will be present within each block and the location of this pixel within the block $\{b_{ij}\}$ will be generated

from a pseudo-random sequence $\{p_{1i}\}$. The polarity of each block will be determined by a second pseudo random sequence $\{p_2\}$. The overall dither pattern will be the product of $\{p_2\}$ and $\{p_{1i}\}$:

$$\begin{cases} x(i,j,k)=1, \textit{ iff } \ p_{1i,j}(k)*p_2(i,j)=1 \\ x(i,j,k)=0, otherwise \end{cases} \tag{5}$$

where x is the pixel intensity, i, j are the block indices, and k is the pixel location within a block.

(a) Top Level (b)One Block (c) Overall Matrix

Fig.6 Multi-scale Measurement Matrix

3.3. Model Assisted Image Reconstruction

An equally important aspect of any CS application is the optimization process to reconstruct the image. The process of spatially modulating the target with an incoming binary dither pattern $\{A_b\}$ can be modeled as:

$$\begin{aligned} y_m &= \sum\left[((A_b \otimes PSF_{IT})X) \otimes PSF_{TR} + \xi(0,\sigma)\right] \\ &= \sum\left[(A_{PSF}X) \otimes PSF_{TR} + \xi(0,\sigma)\right] \end{aligned} \tag{6}$$

where PSF_{IT} and PSF_{TR} are the Point Spread Functions from illuminator to the target and from target to the receiver respectively. As can be seen in (6), instead of $\{A_b\}$, the target X is actually modulated with $\{A_{PSF}\} = \{A_b \otimes PSF_{IT}\}$. Therefore, $\{A_{PSF}\}$ should be used as the measurement matrices in image reconstruction. Accordingly, the accuracy of $\{A_{PSF}\}$ is critical to the success of image reconstruction.

Numerical models such as the EODES imaging model developed in cooperation between HBOI and Metron, Inc. [21] can predict the image under given environmental parameters (attenuation coefficient c and scattering coefficient b, solar irradiance level, distance between illuminator, target and receiver, target reflectance etc.) and system configuration (lens aperture, field of view, laser power etc.). While these types of numerical models are typically used for at-sea performance prediction and to correlate with experiment data for theoretical analysis, this research would propose a new paradigm of incorporating results from model prediction in actual image processing tasks such as image reconstruction for underwater CS imagers.

3.4. Volume Backscattering Reduction

Figure 7 Mirror Polarity Flipping to reduce volume backscattering

Another unique property of the CS based imager is that it enables a new approach to reduce the volume backscattering. When imaging a static scene, the scene geometry and incident laser power will remain unchanged between measurements. Consequently, the backscatter can be modeled as a Gaussian noise with a constant mean. To reduce backscatter, a polarity flipping technique can be used. Each dither pattern is loaded twice, first with mirror "on" corresponds to a digital "1" in $\{p_2\}$, and then with mirror "off" corresponds to a digital "1". The difference of the two readings reduces the backscattering to a zero-mean Gaussian:

$$
\begin{aligned}
y_m &= y_{m+} - y_{m-} \\
&= \sum [A_+ X + \xi(C,\sigma))] - \sum [A_- X + \xi(C,\sigma))] \\
&= \sum [(A_+ - A_-) X + \xi(0,\sigma)]
\end{aligned} \tag{7}
$$

3.5. Overall System Design

After incorporating the multi-scaled measurement matrices design and model-assisted reconstruction, the overall system flow can be summarized in the flowchart in Figure 8 (b): A series of pre-generated binary measurement matrices are loaded onto DMD to modulate the laser beam and illuminate the target plane. The same binary matrices are also sent into radiative transfer model such as EODES model to predict the measurement matrices at the target plane. The predicted measurement matrices consists one input to the image reconstruction process. On the other end, a PMT type "bucket" photon collector records the total target reflections. The PMT voltages are digitized to constitute the second input to the image reconstruction process. The image of the target plane can then be reconstructed with the predicted measurement matrices and the digitized PMT voltages.

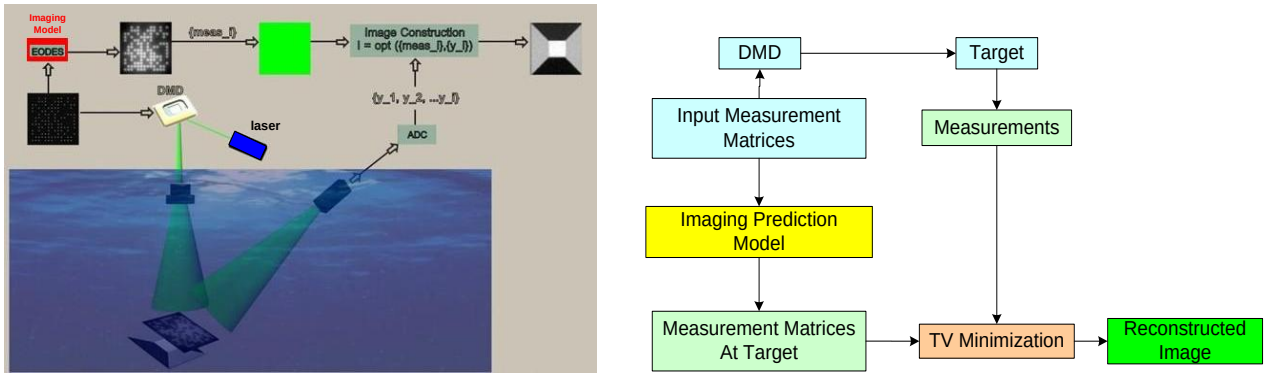

(a) System Operation Description (b) System Flow Chart

Figure 8 Compressive sensing based Underwater Laser Imager

3.6. Advantages of the CS based Underwater Laser Imager

The following are some potential benefits of the proposed design:

Improves system reliability and compactness and reduces system BOM. Like the structured illumination based design, a commercially available solid-state SLM device such as DMD is used to replace bulky mechanical and optical components in the LLS. This helps to improve the system reliability, compactness as well as contributing to BOM reduction. Furthermore, the compressing-during-sampling paradigm requires lower-speed electronics, which in turn improves system noise performance and reduces system BOM.

Good Photon Efficiency/Concentration. Because the CS imager uses the "bucket" photon collector such as PMT like the laser line scan system, the photon efficiency would be better than that of the structured illumination based system.

Intrinsically Encrypted and Robust Process. One interesting aspect of proposed design is that the receiver will need both the measurements as well as the measurement matrices to reconstruct the image. In this sense, CS based imaging can be modeled as an encrypted communication channel. In the distributed imaging and communication environment [24] where the illuminators and receivers are on different platforms, this attribute is highly desirable since both compression and encryption can be realized without any additional hardware. In addition, because each measurement is independent with each other, if certain measurements were lost during the imaging process, as long as the indices of these lost measurements are known, the data loss can be regarded as reconstructing image with increased compression ratio.

Compatible with existing laser/receiver and artifacts mitigation techniques. Of all the components used in the laser line scan system, the proposed system essentially only replaces the scanning mechanism with solid-state SLM device. The laser and PMT developed for LLS can be readily used in CS based imaging system. Additionally, while the aforementioned polarity flipping technique provides a volume scattering reduction method that can help with systems

using CW laser, the test-and-true volume scattering reduction via pulsed laser and range-gated receiver is still valid for CS based imaging system.

Flexibility. In addition to the simplified illuminator design that is highly desirable in distributed underwater imaging applications, the CS based imager shares another feature with the multi-static underwater LLS system in that in turbid water – it does not require direct line-of-sight between target plane and receiver [25]. This is one of the main motivations for adopting an illuminator based SLM over a receiver based approach demonstrated in Rice one-pixel camera.

3.7. Potential Application Scenario for CS based Underwater Laser Imager

One potential application of the CS underwater laser imager is a long-range high-resolution underwater imaging system that integrates the CS imager with an acoustic communication link (Figure 9).

At the front end, the illuminator consists of the laser and , the pre-stored binary measurement matrices are loaded onto DMD to modulate the laser and illuminate the target; The PMT at a local receiver (either co-locate on the same platform as the illuminator or on a different platform) records the total target reflection. Its output is digitized and fed into an acoustic transducer to transmit the data to the remote site. The IOP of the water column and the imaging system parameters will also be updated in addition to the measurement data stream. At the remote site, the same binary measurement matrices together with the IOP data and imaging system parameters are fed into a radiative transfer model like EODES to compute the measurement matrices. These predicted measurement matrices are then used in conjunction with the incoming measurement data stream to reconstruction the target image.

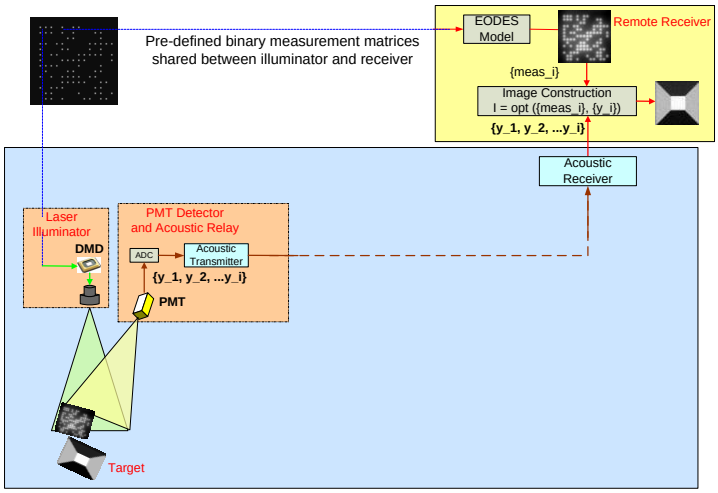

Figure 9 High-Resolution Long-Range Imaging using CS Imager

As described in section 3.6, the communication link in this integrated system is intrinsically encrypted and compressed without requiring additional hardware. The system would takes advantages of the high resolution imaging capability offered by the CS imager as well as the extended communication range achievable via the acoustic link. For example, to reconstruct an image with 256x256 at a 10:1 compression ratio requires about 6000 measurements. If an ADC with 12-bit resolution is used, then to transmit/reconstruct an image with such resolution within 1 second would require a 70kbps communication link. Such a link with a range of several kilometers is achievable using underwater acoustic communication systems [26].

4. SIMULATION AND EXPERIMENT

Simulations were conducted to study various aspects of the proposed CS based imager. The EODES imaging model for near mono-static LLS system was modified for this work. Since the same model was used to predict the measurement matrices to be used in image reconstruction, consideration had to be given to ensure the simulation environment was realistic. As shown in Figure 10, different scattering coefficient *b* (since it has the most significant impact) could be specified for simulation path (red arrows) and model-prediction path (blue arrows) to simulate inaccurate IOP measurements when predicting the measurement matrices using EODES model. Furthermore, noises could be added to simulate both laser variations (Gaussian noise) and PMT system operation (Poisson noise) along the simulation path.

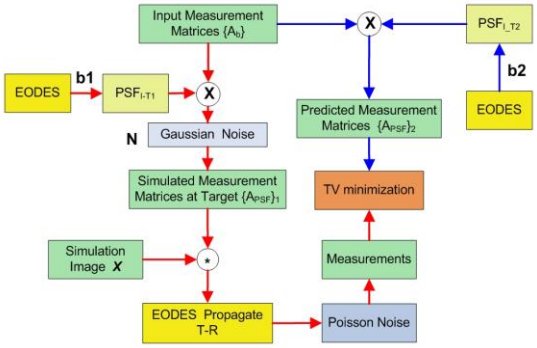

Figure 10 Simulation Flow

During all simulations, the PMT Poisson noise was added in all cases. The results involved other variability (IOP, laser) were also studied. In addition, laser power was set to 1 mW in CS system simulation and 2W in LLS system simulation to take into the consideration that CS imager operates in frame based mode. It should be noted to match the system configuration used in simulating near mono-static LLS, a PMT with telescopic field of view (30 mrad) was used, which was not optimum for CS imager.

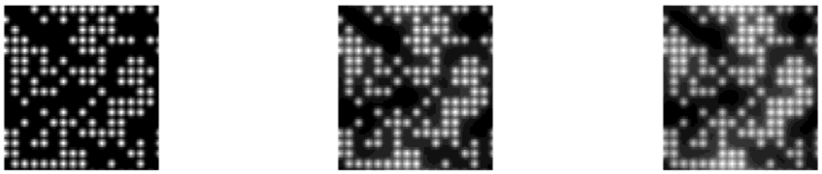

Att. Len=1 Att. Len=5 Att. Len=7

Figure 11 Multi-scale Measurement Matrix

The measurement matrices performance were shown in Figure 11. During the experiment, block size of 4 was used. While the beam spreading increased with longer attenuation length, the beams maintained good separations in all cases.

The comparison between model-assisted reconstruction and reconstruction using binary matrices was presented in Figure 12 (a). At attenuation length=7, using the same number of measurements, the image reconstructed using binary dither pattern was seriously degraded while the results from the model-assisted approach retained good image quality.

Att. Len	Binary	Model Predicted
7	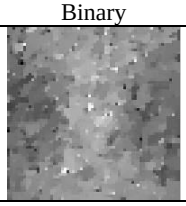	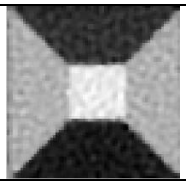

(a) Impact of model predicted measurement matrices

No Polarity Flip	Polarity Flip
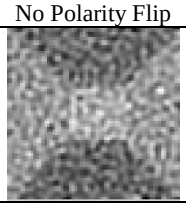	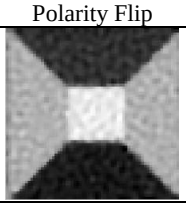

(b) Impact of polarity flip measurement matrices

Figure 12 Impact of Different Measurement Matrices (Using 800 measurements)

The benefit of polarity flip was also demonstrated in the side-by-side comparison of the reconstructed images obtained under the same conditions (Figure 12 (b)).

Next, the images from LLS simulation were compared with the reconstructed images from CS based imager simulations. Simulations were done with a 64x64 images. The reason higher resolution images were not used was due to the memory limitation in handling model-predicted measurement matrices in l_1-magic code. The LLS simulation did not include volume backscattering or solar irradiance. The results were shown in Figure 13. It could be seen that the image quality improved with increasing number of measurements for CS based imager. The image quality of CS imager was in general comparable with that of LLS. One interesting observation was that with increased turbidity CS imagery still maintained good edge sharpness whereas LLS imagery became blurry.

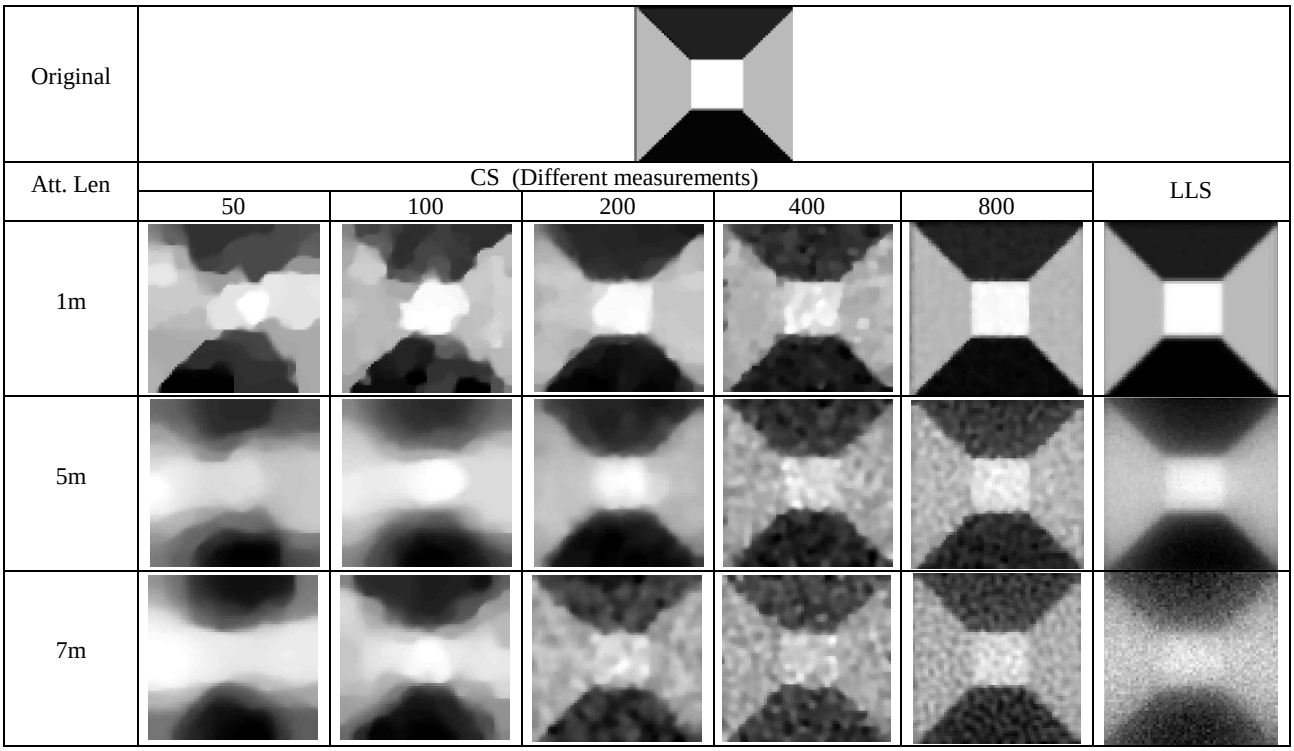

Figure13 Comparison between LLS and CS with different number of measurements

Finally, simulations with environmental variations were conducted. The real scattering coefficient (scattering coefficient used in simulation path) was assumed to be 5% higher than that used to predict measurement matrices. The laser was assumed to contain 5% variation also. As shown in Figure 14, while the results were not as good as those generated without such variations, the degradation was not severe.

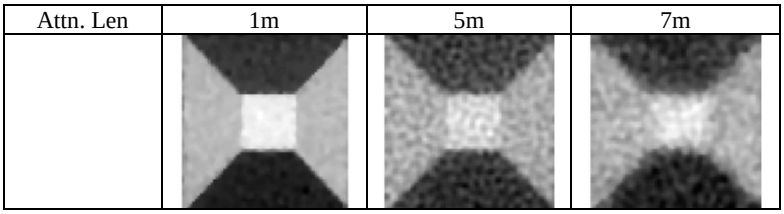

Figure 14 CS images with environment variations

An experiment was also conducted using a simple desktop setup. The measurement matrices were loaded onto a DELL M109S DLP pico projector to illuminate the target board. The PMT output was digitized by a 12-bit ADC. The resulted measurements were used to reconstruct the image. 800 measurements were used to reconstruct images at a resolution of 64x64. The setup and results were shown in Figure 15 (a)-(c). While the setup was primitive, the results validated to a certain degree the effectiveness of the proposed scheme.

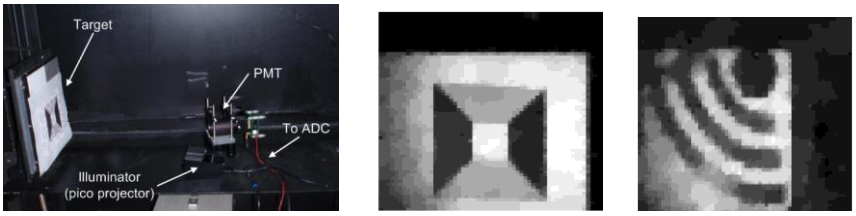

(a) Experiment Setup (b) Geometry (c) Bliptv

Figure 15 Experiment Setup and Results

5. SUMMARY

The proposed compressive sensing based laser serial imager is an attempt to extend the compressive sensing theory to the field of imaging through scattering media, specifically in the underwater environment. The design offers has the potential to improve system reliability, compactness and reduce system cost. As demonstrated in this work and the structured illumination design, Spatial Light Modulators such as DMD will play an important role in such system. Since the CS imager inherits the highly photon efficient "bucket" light collector (PMT) used in the LLS system, it offers better photon efficiency than that of the structured illumination based design.

The paradigm of model-assisted CS is an attractive concept in its own, since it can help to extend CS to other applications involving scattering medium, such as fog, mist, smoke or dust. This polarity flipping based volume scattering reduction can be useful when implementing CW laser based system. Where in a pulsed laser system, this technique can be used in conjunction with the range gated technique to reduce volume backscattering.

While the proposed technique is still in the early stage of the development, the simulation and experimental results did validate the basic concept in the design to a certain degree.

It worth mentioning that while the works currently concentrate on image formation, better speed improvement may be achieved for video by exploiting temporal/spatial redundancy. For example, Sankaranarayanan et al. proposed CS linear dynamical system (CS-LDS) technique [20] that claimed reasonable good video quality with 4% measurement rate.

Finally, it is interesting to compare CS with two other configurations: traditional LLS and structured parallel illumination. A summary of comparisons from several different aspects is presented in Table 1.

Table 1. Comparison of Three Underwater Laser Imaging Techniques.

	CS	**Structured Illumination**	**LLS**
System Design	Using Solid State SLM (DMD) to modulate laser and PMT; Compressing during sampling;	Using Solid State SLM (DMD) to modulate laser and high sensitivity camera based receiver; Compressing after sampling;	Mechanical actuator and high precision prism to direct laser and PMT; Compressing after sampling;
Imaging Method and Speed	Serial Imaging, actual speed depends on compression ratio Additional speed advantage for video.	Parallel Imaging, Should be fastest among all three.	Serial Imaging. Maybe slowest among all three. Scanner speed is gating factor.
Imager Configuration	Can be setup with near mono-static or bi-static configuration. Not require line-of-sight from target to PMT	Requires direct line-of-sight from target to camera; may not be suitable in bi-static configuration.	Can be setup with near mono-static or bi-static configuration. Not require line-of-sight from target to PMT
Photon Efficiency /Concentration	Less than LLS due to the photon loss in SLM, but should be at same level. Pixel photon concentration depends on compression ratio.	Power shared among all active pulses – comprise with imaging speed. Faster speed = lower photon Concentration.	Highest, all incident power used to construct pixel intensity
Motion Artifacts	Platform excursion can be modeled as Gaussian noise in measurements, handles as constraints in image reconstruction.	Misalignments of consecutive SLM pulses induces artifacts. Can be addressed in image synthesis;	Pixel misalignment due to motion. Can be compensated with known platform motion data or deconvolutoin .
Backscatter Mitigation	1) Polarity flipping for CW laser. 2) Pulsed laser and range-gated receiver.	Pulsed laser and range-gated camera	Pulsed laser and range-gated receiver.
Image Reconstruction	Computation intensive optimization is required.	Comparative low intensity image synthesis required.	Minimum additional process required.

6. ACKNOWLEDGEMENTS

This work was conducted under a grant monitored by the US Office of Naval Research and institutional funding from Harbor Branch Ocean Institute.

REFERENCES

[1] J. S. Taylor and M. C. Hulgan, "Electro-Optic Identification Research Program," Proc. MTS/IEEE Oceans '02, Vol. 2, pp. 994-1002, 2002.

[2] J. S. Jaffe, "Extended Range Optical Imaging using One and Two Dimensional Structured Illumination," Optics Express, Vol. 18, pp. 12328-12340, 2010.

[3] D. Donoho, "Compressive Sensing," IEEE Trans. Inform. Theory, vol. 52, pp. 1289-1306, 2006.

[4] E. Candes and T. Tao, "Near Optimal Signal Recovery from Random Projections: Universal Encoding Strategies," IEEE Trans Inform. Theory, vol. 52, pp. 5406-5425, 2006.

[5] S. Chen, D. Donoho, M. Saunders, "Atomic Decomposition by Basis Pursuit," SIAM J. Science Comp., 20, pp. 33-61, 1999.

[6] E. Candes and J. Romberg, "Sparsity and Incoherence in Compressive Sampling," Inverse Problems, vol. 23, pp. 969-985, 2007.

[7] L. Gan, T. Do and T. Tran. "Fast Compressive Imaging using Scrambled Block Hadamard Ensemble". Proc. EUSIPCO, 2008.

[8] M. Duarte, M. Davenport, D. Takhar, J. Laska, T. Sun, K. Kelly and R. Baraniuk, "Single-Pixel Imaging via Compressive Sensing," IEEE Signal Processing Magazine, vol. 25, pp. 83–91, 2008.

[9] R.G. Baraniuk, "Compressive Sensing," IEEE Signal Processing Magazine, vol. 24, pp. 118-121, 2007.

[10] S. Jafarpour, R. Willett, M. Raginsky and R. Calderbank, "Performance Bounds for Expander-Based Compressed Sensing in the Presence of Poisson Noise," Proc. Asilomar Conference on Signals, Systems, & Computers, 2009.

[11] E. Candes and J. Romberg, "Robust Signal Recovery from Incomplete Observations," Proc. ICIP, pp. 1281-1284, 2006.

[12] E. Candes, J. Romberg, and T. Tao, "Stable Signal Recovery from Incomplete and Inaccurate Measurements," Comm. Pure Appl. Math., vol. 59, pp. 1207-1223, 2006.

[13] E. Candes, J. Romberg, and T. Tao, "Robust Uncertainty Principles: Exact Signal Reconstruction from Highly Incomplete Frequency Information," IEEE Trans. Inform. Theory, vol. 52, pp. 489-509, 2006.

[14] l1-magic, [Online], http://www.l1-magic.org.

[15] T. Do, T. Tran, and L. Gan, "Fast Compressive Sampling with Structurally Random Matrices," Proc. ICASSP, pp. 3369 – 3372, 2008.

[16] Dana Dudley, Walter Duncan and John Slaughter, "Emerging Digital Micromirror Device (DMD) Applications," Proc of SPIE, 2003, 4985, 14-25.

[17] J. Ma, "Single-Pixel Remote Sensing," IEEE Geoscience and Remote Sensing Letters, Vol. 6, pp. 199 – 203, 2009.

[18] M. Lustig, D. Donoho, and J. M. Pauly, "Sparse MRI: The Application of Compressed Sensing for Rapid MR Imaging," Magnetic Resonance in Medicine, Vol. 58, pp. 1182 - 1195, 2007.

[19] R. G. Baraniuk and T. P. H. Steeghs, "Compressive Radar Imaging," IEEE Radar Conference, 2007.

[20] A. C. Sankaranarayanan, P. K. Turaga, R. G. Baraniuk1, and R. Chellappa, "Compressive Acquisition of Dynamic Scenes," Proc. Of European Conference on Computer Vision'10, 2010.

[21] T. E. Giddings and J. J. Shirron, "Numerical Simulation of the Incoherent Electro-optical Imaging Process in Plane-Stratified Media," Opt. Eng. 48, 126001 (2009).

[22] F. R. Dalgleish and F. M. Caimi, "Synchronous Laser Line Scanners for Undersea Imaging Applications," Accepted as a book chapter for Taylor and Francis series in Optical Engineering (Laser and Optical Scanning).

[23] http://www.dlp.com.

[24] F. R. Dalgleish, F. M. Caimi, A. K. Vuorenkoski, B. Ramos, W. B. Britton, T. E. Giddings, J. J. Shirron, and C. H. Mazel, "Laser-pulse-dispersion codes for turbid undersea imaging and communications", SPIE, Vol. 7678, 2010.

[25] B. Ouyang, F. R. Dalgleish, A. Vuorenkoski, W. Britton, B. Ramos and B. Metzger, "Visualization for Multi-static Underwater LLS System using Image Based Rendering", submitted to IEEE Journal of Oceanic Engineering.

[26] M. Stojanovic, "Underwater Acoustic Communications," in Encyclopedia of Electrical and Electronics Engineering, John G. Webster, Ed., John Wiley & Sons, 1999, Vol.22, pp.688-698.